Chinese Chemical Letters 32 (2021) 583–586

Contents lists available at ScienceDirect

Chinese Chemical Letters

journal homepage: www.elsevier.com/locate/cclet

Communication

Hydrothermal-assisted grinding route for WS_2 quantum dots (QDs) from nanosheets with preferable tribological performance

Zhi-Lin Cheng*, Lu Ma, Zan Liu

School of Chemistry and Chemical Engineering, Yangzhou University, Yangzhou 225002, China

ARTICLE INFO

Article history:
Received 2 January 2020
Received in revised form 21 January 2020
Accepted 5 February 2020
Available online 5 February 2020

Keywords:
Nanosheets
WS_2
Quantum dots
Tribological performance
Grease

ABSTRACT

The 2D nanomaterials have achieved the superlubrication property whatever in solid or liquid lubrication in recent years. However, whether or not the nanosheets can stably disperse in oils and smoothly enter into the asperity of friction pairs is crucial for exerting the function of antifriction. The structure of 2D QDs is desirable for addressing these issues due to its smaller 3D size. In this study, we developed a facile preparation process for WS_2 QDs with uniform 2 nm size from nanosheets *via* hydrothermal-assisted grinding approach. The structure of the as-obtained WS_2 QDs was determined by a series of characterizations. The results showed that the as-obtained WS_2 QDs exhibited the typical spectrum features of nanosized quantum dot. The results of the tribological performance in grease verified that the average friction coefficient (ACOFs) and wear volume (AWVs) were decreased by 7.89% and 63.90% relative to grease, respectively, exhibiting a preferable friction reducing and wear resistance.

QDs are a class of nanomaterials with size usually smaller than 10 nm, the properties of which are different from bulk or even corresponding bigger nanoparticles. WS_2 QDs have aroused the considerable attentions in the field of light-emitting devices [1], solar cells [2–5], catalysis [6] and biological applications [7] due to owning optical, electronic, and mechanical properties [8–10]. So far, the WS_2 quantum dots have been achieved by many methods, such as hydrothermal [11], mechanical pulverization [12], liquid phase sonication [13], ion intercalation [14], electrochemical exfoliation method [15], *etc*. For example, the recent years have sprung up the bottom-up route for the WS_2 QDs with 6−10 nm size [16], the mechanical exfoliation the WS_2 QDs with an average size of 2.1 nm [17], the individual liquid phase for WS_2 QDs with 3–4.5 nm in deionized water [18] and the solvothermal treatment for the uniform WS_2 QDs with the monolayer thickness and average size of about 3 nm [19, 20]. Encouragingly, the reproducible production of defect-free WS_2 quantum sheets with supper high yield of 20.1 wt% was obtained by the cooperative processing of salt-assisted ball-milling and sonication-assisted solvent exfoliation [21]. The preparation of WS_2 QDs with the size of less than 10 nm was fulfilled from bulk crystals by using a combination of grinding and sonication techniques [22]. However, these routes were of high-cost, complicate-processing and long-sustained features in preparation. Consequently, it is urgent to develop the desirable method to prepare the WS_2 QDs. Furthermore, since 2D inorganic nanosheets as additive were successfully applied in lubricants, they have attracted abundant interests in friction reduction and wear resistance of machinery industry [23–26]. Nevertheless, the WS_2 QDs applied for friction reducing improvement in oils were barely reported.

In this work, we successfully developed a facile exfoliation process for WS_2 QDs from nanosheets *via* hydrothermal-assisted grinding approach. The as-obtained WS_2 QDs were determined by a series of characterizations. The preparation mechanism of WS_2 QDs was proposed. The tribological properties of the as-exfoliated WS_2 QDs in grease were intensively evaluated by the reciprocating ball-on-disk mode.

The self-made 2.0 g WS_2 nanosheets [27] were dispersed in 30 mL phosphoric acid solvent, and allowed magnetic stirring for 10 min at room temperature. After being mixed evenly, they were transferred into a 50 mL Teflon-lined stainless steel autoclave, and successively heated in a homogeneous reactor at 200 °C for 6 h under 10 rpm of rotation speed. After the ending, the autoclave was cooled down to the room temperature. The precipitate was collected by centrifugation with 10,000 rpm for 5 min, followed by washing at least five times with absolute ethanol for removing residual phosphoric acid. Then, the resulting sample was ground in a mortar for 1 h along with periodically adding 1 ml absolute

* Corresponding author.
E-mail address: zlcheng224@126.com (Z.-L. Cheng).

https://doi.org/10.1016/j.cclet.2020.02.002

ethanol solvent. After the ending, the suspension was collected by centrifugation with 10,000 rpm for 5 min, followed by washing at least five times with absolute ethanol, denoted WS_2 QDs.

Fig. 1 displays the TEM, HRTEM and selected area electron diffraction (SAED) images of the as-exfoliated WS_2 nanosheets and QDs. Apparently, the size of the as-exfoliated WS_2 QDs is evidently smaller than WS_2 nanosheets (Figs. 1a and d). This suggests that the structure of WS_2 nanosheets were destroyed to some extent in hydrothermal process. The HRTEM images definitely demonstrates that the lattice spacing of WS_2 nanosheets and QDs is about 2.7 Å, which is associated to the (100) plane [28]. Nevertheless, the thickness of the former is approximately 3.15 nm (11–12 layers) and that of the latter is rarely elusive due to having too small size (Figs. 1b and e). The SAED pattern distinctly shows that WS_2 nanosheets and QDs are of the six-fold symmetric structural feature, and the highly ordered and parallel lattice fringes of latter are more obvious due to seriously overlying nanoparticles than the former (Figs. 1c and f). These results are assumed that the lateral size of nanosheets is reduced and the pulverization of WS_2 nanosheets is transformed into QDs [29]. Figs. 1g and h show the AFM images of the as-exfoliated WS_2 nanosheets and QDs. As marked in Fig. 1g, the thickness of WS_2 nanosheets is about 3.5 nm, which is consistent to the HRTEM result. Further, the thickness of WS_2 quantum dots is less than 0.8 nm (Figs. 1h and i). This result corroborates the conversion from nanosheets to quantum dots. We suppose that the strong coordination complexes of phosphate radical can destroy the van der waals force of interlayer and the in-plane covalent bond of WS_2 at first-stage hydrothermal process and subsequently the second-stage grinding processing in the ethanol solvent can effectively prevent the restacking between the layers [30,31].

Fig. 2 gives the XRD patterns, EDS, Raman and UV–vis spectra of WS_2 nanosheets and quantum dots. As shown in Fig. 2a, the as-exfoliated WS_2 nanosheets contains the stronger peak at (002) plane and weaker peaks at (004), (101), (103), (006), (105), (106) and (112) planes, which is compatible to the few-layer WS_2 nanosheets [32]. However, as for the WS_2 QDs, the typical stronger (002) plane is disappeared, and there exist barely three very weak feature peaks. This result is in good agreement with the reported

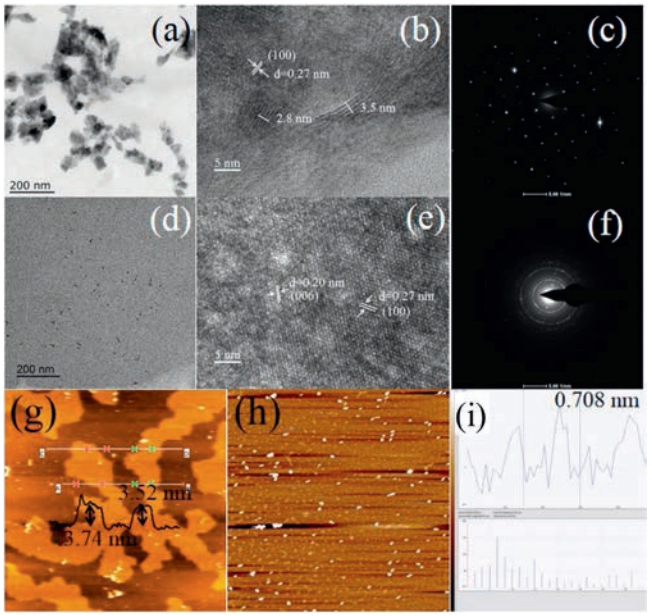

Fig. 1. TEM (a, d), HRTEM (b, e), SAED (c, f) and AFM (g, h) images of WS_2 NSs (a, b, c, g) and WS_2 QDs (d, e, f, h); the height image of WS_2 QDs.

monolayer TMD quantum dots [33], indicating that the as-obtained WS_2 QDs are of the nanosized structure of quantum dots. The EDS spectrum (Fig. 2b) demonstrates that the as-obtained WS_2 QDs only contain the W and S elements, and the W/S atom ratio is nearly 1:2, matching to the element composition of WS_2 [32]. As shown in Fig. 2c, the two typical peaks (E and A_{1g}) are assigned to the in-plane motion of the W and S atoms and the out-of-plane vibrations of the S atoms, respectively [34]. The characteristic modes E and A_{1g} of WS_2 nanosheets locate at 348.61 and 417.5 cm^{-1}, respectively. Compared to WS_2 nanosheets, the E peak (352.34 cm^{-1}) of the WS_2 QDs is significantly weakened and has an obvious blue shift. This is attributed to the structure change of quantum dots in the reduction of thickness and lateral size [35]. Fig. 2d shows the UV–vis absorption spectra of the WS_2 NSs and QDs suspension in ethanol. The WS_2 NSs have the characteristic absorption peaks located at 638 nm (A, 1.94 eV), 275 nm (B, 4.51 eV) and 236 nm (C, 5.25 eV). For the WS_2 QDs, it is found that there are two weak absorption bands at around 264 nm (B, 4.70 eV) and 213 nm (C, 5.82 eV). A slight blue shift occurring in absorption peaks is assumed to arise from the reduction of lateral dimension of the nanosheets into nano size.

Fig. 3 shows the photoluminescence spectra (PL) of WS_2 nanosheets and quantum dots at different excitation wavelengths ranging from 240 nm to 380 nm. For few-layer WS_2 NSs, the two broad peaks lie at approximately 597.4 and 724.2 nm under 532 nm excitation wavelength (Fig. 3a), which should be originated from direct band gap of WS_2 nanosheets [36]. Nevertheless, the PL emission spectra of WS_2 QDs depending on the excitation wavelength (Fig. 3b) corroborate that the maximum emission at 340 nm is observed at an excitation wavelength of 280 nm, which is consistent to that of WS_2 quantum dots [37]. As the excitation wavelength increases, the emission pattern shifts to higher wavelength. The reason is that the surface state is similar to a molecular state and the size effect is as result of quantum dimension, both of which contribute to the complexity of the excited states of QDs. Moreover, the WS_2 QDs ethanol solution displays a yellow color in daylight, but emits the blue light under UV irradiation at 365 nm (3.40 eV) (Fig. 3b inset). This excitation wavelength-dependent PL also may be attributed to the presence of oxygen moieties adsorbed at the edges.

Fig. 4 shows the XPS and FT-IR spectra of WS_2 QDs As shown in the XPS survey spectrum (Fig. 4a), apart from W and S elements, other elements exhibit a pristine chemical state. The existence of C and O are ascribed to the tiny oxidation of W edges and the adsorption of CO_2 on the surface of quantum dots in air [24]. The bands at 31.68 and 33.83 eV (approximately 2.3 eV) are assigned to W $4f_{7/2}$ and W $4f_{5/2}$, respectively, and the W $5p_{3/2}$ peak is observed at 37.03 eV (Fig. 4b). Likewise, the coexistence peaks of S $2p_{3/2}$ and S $2p_{1/2}$ appear at around 161.38 and 162.53 eV, which are attributed to the -2 valence state of S atoms (Fig. 4c) [38]. The functional groups on the WS_2 QDs are also identified by FT-IR spectra (Fig. 4d). In contrast to nanosheets, the peaks at 1433 cm^{-1} and 1634 cm^{-1} are assigned to the C=C, and the peaks at 1080 cm^{-1} and 827 cm^{-1} are assigned to the C=O [39]. The appearance of these peaks suggests that the surface of WS_2 QDs nanoparticles has a great deal of the active sites.

As shown in Fig. S1 (Supporting information), upon the content of the WS_2 QDs in grease up to 2.0 wt%, the average friction coefficient (ACOF) and wear volume (AWV) are decreased by 7.89% and 63.90% relative to grease, respectively. The AWV lubricated by the as-exfoliated WS_2 QDs-based grease is significantly reduced by 82.89% and 76.45% relative to grease and bulk WS_2-based grease, respectively. To our best knowledge, the antifriction and antiwear mechanism of 2D nanomaterials is generally considered to the formation of the low friction-coefficient tribo-film on the surface of friction pairs. The smaller size nanoparticles smoothly enter into

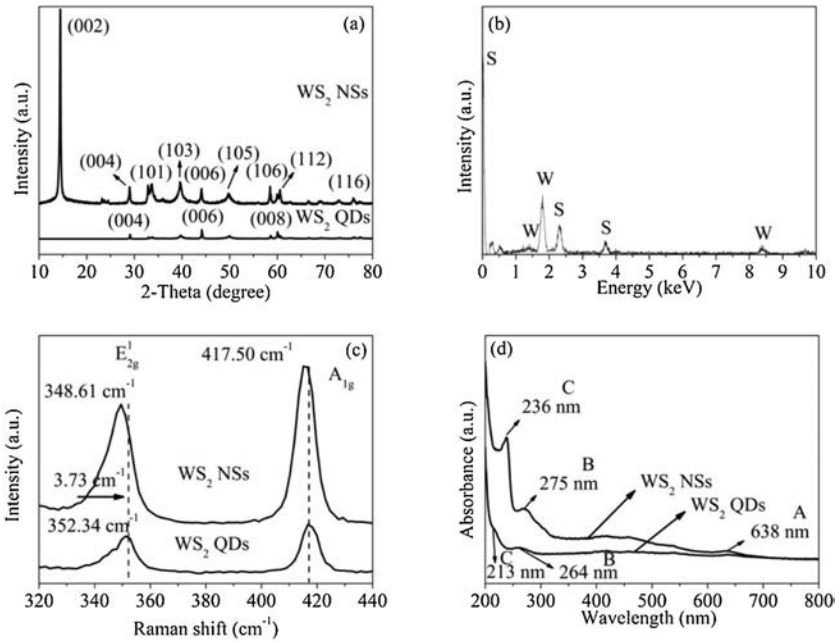

Fig. 2. XRD patterns (a), EDS(b), Raman (c) and UV–vis spectra (d) of WS_2 NSs and QDs.

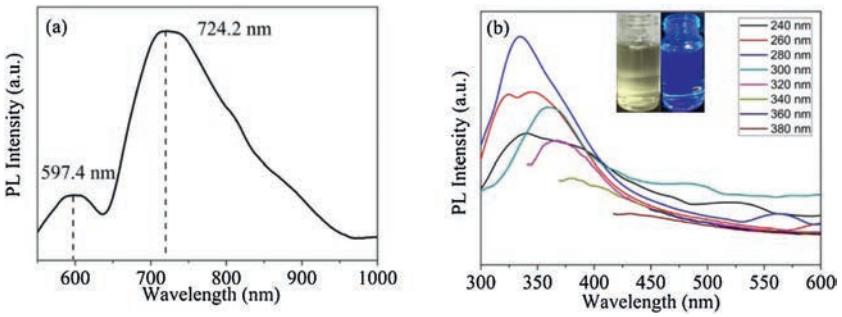

Fig. 3. PL spectra of WS_2 NSs (a) and QDs (b).

the gaps and properly fill the valleys between the asperities of the sliding steel pair. Therefore, the advantage of WS_2 QDs is difficult to be fully squeezed out of the contact area due to owning the smaller size than nanosheets in three dimensional directions [40].

In summary, we successfully prepared WS_2 QDs *via* the hydrothermal-assisted grinding of nanosheets. The tribological performance indicated that the as-obtained WS_2 QDs could significantly improve the friction and wear resistance of grease, which exhibited the desirable application prospect.

Declaration of competing interest

The authors declare that they have no known competing financialinterestsor personal relationships that could have appeared to influence the work reported in this paper.

Acknowledgments

This work was funded by Jiangsu Province Six Talent Peaks Project (No. 2014-XCL-013) and Jiangsu Industrial-academic-research Prospective Joint Project (No. BY2016069-02). The authors also acknowledge the Project Funded by the Priority Academic Program Development of Jiangsu Higher Education Institutions and Top-notch Academic Programs Project of Jiangsu Higher Education Institutions (No. PPZY2015B112). The data of this paper originated from the Test Center of Yangzhou University.

Appendix A. Supplementary data

Supplementary material related to this article can be found, in the online version, at doi:https://doi.org/10.1016/j.cclet.2020.02.002.

References

[1] S.X. Cao, C. Zhao, L.L. Peng, Mater. Lett. 164 (2016) 452–455.
[2] Y.X. Li, M. Peng, W. Zhou, X. Gong, et al., J. Mater. Chem. A 5 (2017) 21452–21459.
[3] Z.L. Li, X.J. Zhao, C.B. Huang, et al., J. Mater. Chem. C 7 (2019) 12373–12387.
[4] W.W. Ma, W.J. Li, R.Y. Liu, et al., Chem. Commun. 55 (2019) 7486–7489.
[5] Z.J. Wang, X.J. Zhao, Z.Z. Guo, et al., Org. Electron. 62 (2018) 284–289.
[6] G.Q. Han, Y.R. Liu, W.H. Hu, et al., Mater. Chem. Phys. 167 (2015) 271–277.
[7] J. Hao, L. Huang, X. Gong, ACS Sustain. Chem. Eng. 7 (2019) 18213–18227.
[8] Y.Q. Wang, F. Yu, M.Y. Zhu, et al., J. Mater. Chem. A 6 (2018) 2011–2017.
[9] W. Li, Z.L. Cheng, Z. Liu, RSC Adv. 6 (2016) 110866–110873.
[10] K. Peng, L.J. Fu, H.M. Yang, et al., Nano. Res. 10 (2017) 570–583.
[11] W.X. Yin, D. He, X. Bai, et al., J. Alloys. Compd. 786 (2019) 764–769.
[12] S. Pal, K.K. Tadi, P.M. Sudeep, et al., Mater. Chem. Front. 1 (2017) 319–325.
[13] S. Zhang, J. Li, E.K. Wang, J. Mater. Chem. B 5 (2017) 2609–2615.
[14] L.X. Lin, Y.X. Xu, S.W. Zhang, et al., ACS Nano 7 (2013) 8214–8223.

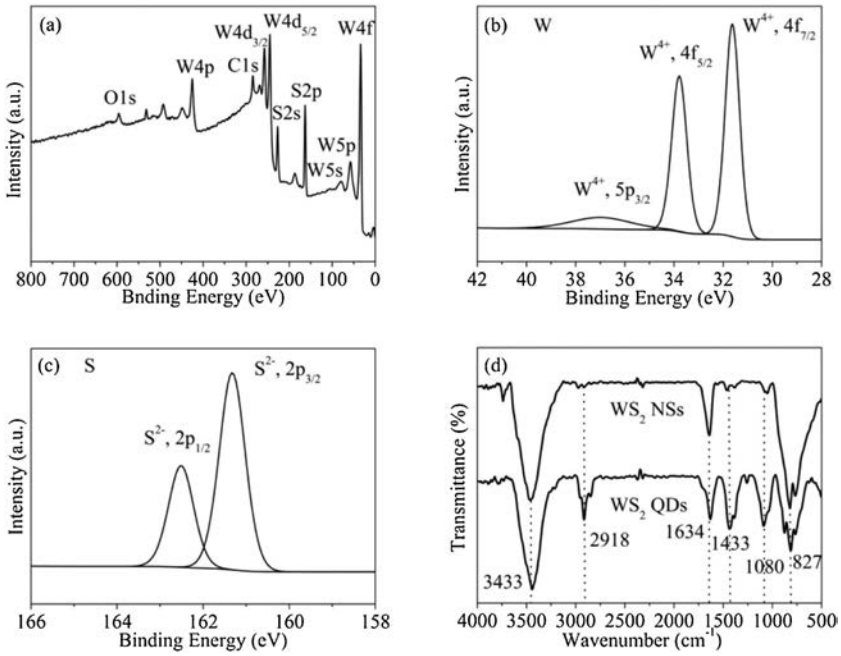

Fig. 4. XPS of WS_2 QDs: (a) Survey scan, (b) elemental W 4f, (c) S 2p. (d) FT-IR spectra of WS_2 NSs and QDs.

[15] M.O. Valappil, A. Anil, M. Shaijumon, et al., Chem. Eur. J. 23 (2017) 9144–9148.
[16] D.R. Hang, D.Y. Sun, C.H. Chen, et al., Nanoscale Res. Lett. 14 (2019) 271–286.
[17] Y.M. Xu, L.H. Yan, X.Y. Li, et al., Sci. Rep. 9 (2019) 2931–2940.
[18] S. Sharma, S. Bhagat, J. Singh, et al., J. Mater. Sci. 52 (2017) 11326–11336.
[19] Y.H. Yan, C.L. Zhang, W. Gu, et al., J. Phys. Chem. C 120 (2016) 12170–12177.
[20] S.J. Xu, D. Li, P.Y. Wu, Adv. Funct. Mater. 25 (2015) 1127–1136.
[21] C.C. Han, Y. Zhang, P. Gao, et al., Nano Lett. 17 (2017) 7767–7772.
[22] X. Zhang, Z.C. Lai, Z.D. Liu, et al., Angew. Chem. Int. Ed. 127 (2015) 5515–5518.
[23] Z.L. Cheng, W. Li, P.R. Wu, et al., Ind. Eng. Chem. Res. 56 (2017) 5527–5534.
[24] Z.X. Zhong, Y.T. Peng, H.J. Lang, Nanoscale 10 (2018) 1855–1864.
[25] Z.X. Zhong, Y.T. Peng, H.J. Lang, et al., ACS Appl. Mater. Interfaces 10 (2018) 8214–8224.
[26] W.L. Zhang, Y.L. Cao, P.Y. Tian, et al., ACS Appl. Mater. Interfaces 8 (2016) 32440–32449.
[27] L. Ma, Z. Liu, Z.L. Cheng, Ceram. Int. 46 (2020) 3786–3792.
[28] L.H. Yuwen, H. Yu, X.G. Yang, et al., Chem. Commun. 52 (2015) 529–532.
[29] Z.L. Cheng, Y.C. Kong, Z. Liu, ACS Sustain. Chem. Eng. 7 (2019) 19770–19778.
[30] P.R. Wu, Z. Liu, Z.L. Cheng, ACS Omega 4 (2019) 9823–9827.
[31] L.Q. Zhong, X. Gong, Soft Matter 15 (2019) 9500–9506.
[32] Z.L. Yan, L.J. Fu, H.M. Yang, et al., J. Hazard. Mater. 344 (2018) 1090–1100.
[33] M. Zhou, Z.L. Zhang, K.K. Huang, et al., Nanoscale 8 (2016) 15262–15272.
[34] A. Bayat, E. Saievar-Iranizad, J. Lumin. 185 (2017) 236–240.
[35] H. Li, F. Xie, W. Li, et al., RSC Adv. 6 (2016) 105222–105230.
[36] M. Baby, K.R. Kumar, Mater. Sci. Tech. Lond. 35 (2019) 1416–1427.
[37] C. Backes, B.M. Szydlowska, A. Harvey, et al., ACS Nano 10 (2016) 1589–1601.
[38] Y. Wang, Y. Liu, J.F. Zhang, et al., Sci. Adv. 3 (2017) 1701500.
[39] F. Huang, J.K. Jian, R. Wu, J. Mater. Sci. 51 (2016) 10160–10165.
[40] Z.L. Cheng, X.X. Qin, Chin. Chem. Lett. 25 (2014) 1305–1307.